FACTA UNIVERSITATIS
Series: **Mechanical Engineering** Vol. 19, Nº 4, 2021, pp. 681 - 704
https://doi.org/10.22190/FUME210331040N

Original scientific paper

INVESTIGATION OF THE GLUED INSULATED RAIL JOINTS APPLIED TO CWR TRACKS

Attila Németh, Szabolcs Fischer

Department of Transport Infrastructure and Water Resources Engineering,
Faculty of Architecture, Civil Engineering and Transport Sciences,
Széchenyi István University, Hungary

Abstract. *This article summarizes the research results related to our own conducted extensive laboratory tests of polymer composite and steel fishplated glued insulated rail joints (GIRJs), namely axial tensile tests as well as vertical static and dynamic tests. The investigation dealt with the examination of GIRJs assembled with steel and special glass-fiber reinforced plastic (polymer composite) fishplates, both of them for CWR railway tracks (i.e. so-called gapless tracks or, in other words, railway tracks with continuously welded rails). The exact rail joint types were MTH-P and MTH-AP, consistently. The MTH P types have been commonly applied for many years in the CWR tracks in Europe, mainly in Hungary. The MTH-AP rail joints consist of fishplates that are produced by the APATECH factory (Russia). They are made of a fiberglass-amplified polymer composite material at high pressure and controlled temperature. This solution can eliminate electrical fishplate lock and early fatigue failures just as it can ensure adequate electrical insulation. The advantage of such rail joints can be that they are probably able to ensure the substitution of the glued insulated rail joints with relatively expensive steel fishplates currently applied by railway companies, e.g. Hungarian State Railways (MÁV). The aim of the mentioned research summarized in this paper is to formulate recommendations on technical applicability and on the technological instructions that are useful in everyday railway operation practice on the basis of the measurements and tests carried out on rail joints in laboratory.*

Key Words: *Glued Insulated Rail Joint, Fishplate, Polymer Composite, Steel, Laboratory Test*

Received March 31, 2021 / Accepted May 12, 2021
Corresponding author: Szabolcs Fischer
Department of Transport Infrastructure and Water Resources Engineering, Faculty of Architecture, Civil Engineering and Transport Sciences, Széchenyi István University,
H-9026 Győr, Egyetem tér 1., Hungary
E-mail: fischersz@sze.hu

1. INTRODUCTION

In the 21st century the railway transportation will be an increasingly important task related to the developed world and society. It started in the 19th and the 20th century with enormous railway construction procedures all over the world.

In the past, the main tasks that had to be solved were a high traction force of the locomotives and other hauling vehicles, transition from the steam to diesel and electric hauling as well as a higher and higher speed demand of the vehicles, etc. Nowadays the environmental friendly technologies (e.g. lower pollution, lower energy demand, green and greener energy for operation, etc.) and the economic solutions (cost efficient with the lowest life cycle costs, even higher lifetime, sustainability, etc.) came to occupy the foreground [1].

In relation to the above-mentioned technologies and technical solutions, we can mention some special ones such as application of noise and vibration damping layers and elements [2–6]; ensuring lower stress in the railway permanent ways' that result and ensure lower elastic and plastic deformation in the track as well as in the layer structure [7–8]; techniques which provide special work processes, e.g. tamping of wide sleepers or side tamping that does not disturb the dense, compacted sub-ballast layer [9–10]; new and newer technologies ensuring decreased dynamic effects that can result in subsidiary failures (maybe cracking, fracturing, breaking) in the tracks' elements [11]; minimizing the wear of track elements (mainly the rails') [12] and lowering the ballast breakage [13–16]. The determination of the geometrical deterioration process is also quite important [17–18] for the ability to predict maintenance work.

Other "trends" can be found regarding the development of railway infrastructure: the improvement of railway network in the aspect of interoperability across the state borders [19–20], accurate surveying of railway tracks, switches and crossings [21–22] as well as checking and measurement of visibility triangles at grade crossings [23].

In the case of dealing with railway infrastructure, the railway traffic, its safety can be also discussed. There are improved, special fuzzy-logic methods and algorithms for safety evaluation [24].

Although it is not strictly related to railway engineering (transport infrastructure part), it is worth mentioning the risk management on railway projects [25], where risk is to be taken into consideration in planning, construction and maintenance phases: Pareto analysis can be applied.

Of course, the above mentioned aspects are not the only ones that can be taken into consideration in relation to the developed railway transportation and railway infrastructure, mainly in the 21st century. It can be assumed that more and more brand new technology and technical improvements will be announced and introduced into this area of transportation because of the demand for the 'best' or high-tech solutions in the future.

This paper deals with a possible new direction of the railway development. In Chapter 2 the authors introduce the basis, the base problems related to the topic of their research. They detail why it is important to consider the application of modified, modern structural elements (e.g. polymer composite fishplates), regarding aspects of CWR tracks (tracks with continuously welded rails) as well as signaling and processing (safety) system related to safe railway traffic.

2. Technical Background, Literature Review

Based on railway maintenance experiences of Hungarian State Railways (MÁV) as well as Raaberbahn, Győr-Sopron-Ebenfurth Railway (GYSEV), glued insulated rail joints prefabricated with steel fishplates need a lot of maintenance source due to rail deformations. The other main problem is a false (railway control) signal due to rail end failures (e.g. creasing, end post cracking, etc.). All this leads to the railway capacity restriction. In Hungarian practice, three rail systems (i.e. rail profiles) were considered for new constructions and rehabilitations as well as for renewal, in the application of polymer composite fishplated glued insulated rail joints: MÁV 48, 54E1 (i.e. UIC 54) and 60E1 (i.e. UIC 60) rail profiles. The main criterion for the choice of rail quality and rail profile should be the railway traffic (axle load, speed, etc.). It means the rails should fulfill requirements as bended-sheared structures with elastic bedded sleepers or elastic bedded RC slabs, etc. Besides, their wear resistance has to be high enough.

The opportunities to connect (join) rails are the following: application of fishplated rail joints, rail welding, and rail expansion devices [26–27]. Basically, the rail joints with fishplates can be set up as (i) traditional fishplated rail joints without any insulation and adhesive material (they are applied in normal 'gapped' railway permanent ways mainly without electric hauling and without special electric railway signaling and processing (safety) systems; (ii) traditional fishplated rail joints with electric insulation (insulated rail joints with fishplates) but without adhesive material (gluing) in normal 'gapped' railway permanent ways as well as in CWR tracks mainly with electric hauling and with special electric railway signaling and processing (safety) systems; (iii) glued insulated rail joints with electric insulation and adhesive material mainly in CWR tracks (Fig. 1). (It has to be mentioned that application of glued insulated rail joints is also allowed in 'gapped' tracks, but it is not a common solution due to its high costs.)

Fig. 1 Glued insulated rail joint assembled by polymer composite fishplates

From other point of view, the fishplated rail joints can be supported or suspended joints [26–27]. The supported rail joints fit only to wooden/timber and synthetic sleepers, but the suspended rail joints can be applied with sleepers produced of any material (i.e. wooden/timber, concrete, reinforced concrete, pre-stressed reinforced concrete, steel, synthetic).

The cross sectional geometry of the fishplates can be seen in Fig. 2. The cross sections of fishplates for glued insulated rail joints are similar to the common flat fishplates, but the main difference between them is that they fill out the space until the rail web while the outer sides of the fishplates are flat, smooth. This geometry provides that they have a higher moment of inertia than the common flat fishplates. The lengths of fishplates have two common values: the 4-hole types are 650 mm long and they are applied to the supported rail joints; the 6-hole types are 900 long and they fit to the suspended rail joints.

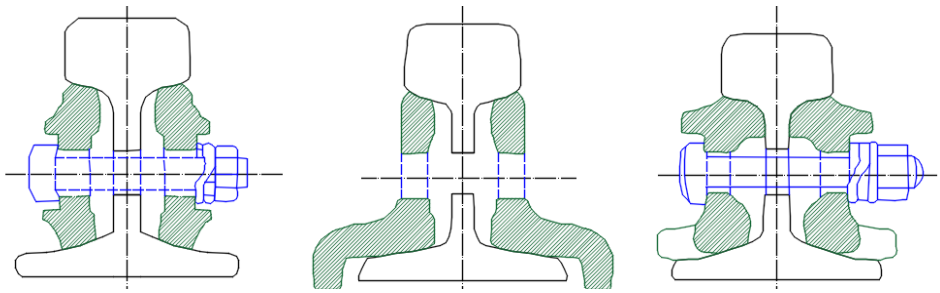

Fig. 2 Common cross sections of fishplates (left: common flat fishplate, middle: angled fishplate, right: bone shape fishplate) (on the basis [27])

Insulated rail joints are special types of fishplated rail joints where the rail ends are insulated from each other. In this way a metallic connection cannot arise either at the rail ends or *via* fishplates [27]. The role of the rail connections (rail joints) is to ensure the continuity of the rails without vertical and horizontal 'steps' as well as without horizontal angle.

The glued insulated rail joint solution with polymer composite fishplates can eliminate failure caused by early fatigue just as it can ensure electrical conduction insulation between the rails to be connected. One of the advantages of such rail joints is the 'exchange' possibility of the glued insulated rail joints (with common steel fishplates) currently applied by MÁV. It is important to note that with the precise construction process (e.g. size of the rail end gap) in the context of the rail joint's assembly, the design of the bedding layer with sufficient compactness (dense) greatly influences the change of the condition of the glued insulated rail joints.

These rail connections are the weak points of the railway track because their fishplates can compensate only for 60% of the moment of inertia of the original rail profile. The wheel, while passing the gap between the rail ends, hits the forthcoming rail end, which is disadvantageous for the whole railway super- and substructure as well as for the railway vehicle. Dynamic effects are much higher in the case of vertical and/or horizontal steps (and angles) than in the case of rail joints without geometrical failures [28]. It has to be mentioned that lower bending stiffness of fishplates causes a higher rail deflection, or even a permanent deformation of rail ends. Such rail joints are characterized by the impact angle between both the connected rails, which, as a consequence, causes impact forces.

Glued insulated rail joints can be applied in suspended and supported joints depending on their type in the case of value of sleeper space and wheel/axle load on given railway tracks. High tensile strength bolts have to be applied to press fishplates and rail(s) together. In this way, a significant high friction force can be achieved between the fishplates and rails (rail webs). It causes that the high axial forces in the rails cannot open the rail joints (i.e. there

is not any relative movement/displacement between the fishplates and rails; or, in other words, the gap between the rail ends does not open compared to the original value). Plastic profile lining (plate) is incorporated between rail ends to be able to achieve adequate electric insulation in this location, too [26–27].

Glued insulated rail joints can be produced and assembled in factory as prefabricated 'elements' with given rail length values as well as on site, where they are assembled from collected parts [27]. It can be stated that the quality of glued insulated rail joints that produced in factory circumstances is better than the pieces made on site.

As mentioned earlier, there are several relevant problems with glued insulated rail joints [26–27]: (i) railway track geometry faults (results of normal geometrical deterioration of railway tracks); (ii) mechanical/structural failures (due to rolling contact fatigue or fracture of one/some of the elements, i.e. rail, fishplate, bolt; etc.); (iii) failures based on electric insulation problems (i.e. trouble in signaling and processing (safety) systems) due to seeable or non-seeable reasons; (iv) other failures generated due to the (i)…(iii) original problems (water pockets below the support sleepers, etc.). The main reason for application and preferring of glued insulated rail joints with glass-fiber reinforced fishplates is related to the above mentioned (iii) problems. However, the mechanical/structural failures are also important but they are not the general ones. This solution avoids the failures because of the main electric insulation troubles; its basement is the fact that glass-fiber reinforced plastic (polymer composite) material is an electric insulator. In the international literature there are many examples dealing with the topic of insulated and glued insulated rail joints' failures. In the following paragraphs the authors summarize the main consequences from their literature review, regarding and focusing on the relevant aspects. It can be noted that sandwich [29] and composite, laminated structures and products [30] are applied in a very wide range of industry.

In the case of rail joints, the damage is due to a relatively low moment of inertia of the fishplate pair (compared to the whole rail profile) [31] as well as the evolved high stresses that can result in plastic deformation and lipping in the rail steel [32–35]. The lipping phenomenon is a typical failure mode (plastic deformation) at the rail ends because of the 'closing' of the rail heads and passing wheels. The other significant damages, namely, failure modes that are prone to happen, are summarized in the following list [36]: battering, shelling and metal flow of rail end; endpost battering, delamination; cracked joint bar (fishplate); railhead spalling; chipping at rail end and gage corner; railhead crushing; opening (pull apart) of insulated rail joint; dipping of insulated rail joint.

The maintenance cost of rail joints is relatively high; it is critical from the aspect that avoiding of glued insulated rail joints can be solved in a very complicated manner in CWR tracks. It would need difficult solutions to be able to operate modern railway signaling and processing system [31]. The modified rail head geometry (in longitudinal direction, i.e. rounded/offset rail end) is able to decrease the arising stresses and to increase rail joint lifetime [37–38]. The evolution of lipping phenomenon can be hindered by application of higher rail steel qualities and/or rails with heat-treated heads [32–33]. The choosing of adequate adhesive materials influences the deterioration rate [32, 35] while the rail end post with appropriate material and thickness is a critical point [32]. Next to them, the significance of the gluing pattern and the applied adhesive quantity is relatively high [37].

3. Applied Methods, Main Characteristics of Rail Joints and Carried out Laboratory Tests

3.1. Applied methods

There is currently no valid standard that contains requirements related to glued insulated rail joints assembled with glass-fiber reinforced fishplates. The specifications and parameters of the European pre-standard (WG18/DG11) [39] were adopted and applied for the authors' laboratory tests. This pre-standard has parameters and testing methodologies only for glued insulated rail joints with steel fishplates. However, in international literature there are more connected and relevant standards and specifications, like AS 1085.12:2002 standard [40] and Austrian Railways' technical specification [41]. Yet, these could not be used in the authors' research due to the main differences between polymer composite and steel materials. Steel fishplated structures have significant lower deformations than others assembled with plastic ones because e.g. the high difference in Young-moduli as well as bending stiffness values.

MTH-AP type fishplates can be used in CWR tracks as joint bars in suspended rail joints only in the case of temporary purposes. It means that if a permanent steel fishplated glued insulated rail joint is damaged and it has to be replaced/exchanged, glass-fiber fishplates are able to be installed without adhesive but they can be kept at that place for 6 months at most while the highest allowed speed is 120 km/h [42]. After 6 months, they must be replaced with new, steel fishplated GIRJs. One of the purposes of the research is to investigate in the period between 2015 and 2020 as well as some years earlier (i.e. between 2010 and 2012) (detailed in [38]) whether the MTH-AP fishplates were able to be utilized in CWR tracks or not.

Based on the previously mentioned specifications, the authors planned and conducted more tests: (i) in laboratory; (ii) on site (i.e. in real tracks); (iii) they made FE models and have run 2D simulations.

The laboratory test parameters were defined in accordance with the following standards and specifications: (i) axial pulling tests considering ΔT_{rail}=90 °C (ΔT_{rail} is the change in rail temperature in [°C]) according to D.12/H. Hungarian prescription [43]; (ii) axial pulling tests with the consideration of ΔT_{rail}=50 °C according to WG18/DG11 pre-standard [39]; (iii) static and dynamic bending tests according to WG18/DG11 [39].

It has to be noted that axial pulling tests were only conducted for the higher ΔT_{rail} value while the static and dynamic bending tests were performed for more cases than the European pre-standard required.

For the laboratory tests the rail joints were assembled with the application of two types of adhesives (notation 'A' or 'B' refer to the type of adhesive).

The main characteristics of the tested specimens are detailed in Chapter 3.2.1.

Even in the axial pulling tests as well as in the static and dynamic bending tests the authors have applied data analysis and process with the help of MS Excel software. The main evaluations are based on engineering and scientific aspects and methods. The authors have tried to formulate the results and the main conclusions from the point of view of their being able to be used in real applications, under real circumstances. Up to now there is no published, useful, extensive literature which can be adequate for the glued insulated rail joints with special polymer composite fishplates.

3.2. Main characteristics of the rail joints and the conducted laboratory tests

3.2.1. Main characteristics of the rail joints

In this chapter the main properties of the elements of the tested rail joints are specified. It means that the authors give only the relevant ones, not all the available data.

Rails: for each of the assembled specimens (for axial pulling tests as well as static and dynamic bending tests) 'old' and used rail pieces were applied. It means that they had a relatively low traffic loading in the past; in this way they did not have a significant wear in any direction. For the tested rail joints MÁV 48, 54E1 and 60E1 (in the following: rail profiles 48, 54 and 60 abbreviations are also applied, respectively) rail profiles were utilized. Because all the profiles are standard ones, the geometrical data can be found in standards (e.g. MSZ EN 13674-1 standard [44]) and data sheets (e.g. D.54 specification of MÁV [45]) or in technical books [36].

Fishplates: steel fishplates were MTH-P types, the glass-fiber reinforced (polymer composite) fishplates were MTH-AP types (produced by the APATECH factory in Russia). They all are 900 m long and 6-hole fishplates with the hole geometry related to Hungarian standard [42–43, 45]. The main parameters of the fishplates can be found in data sheets of the producers (they cannot be reached on the internet; the details can be found in [38]).

Fishplate bolts were M27 8.8 (in the case of 60 rail profile) and M24 8.8 (in the case of 54 and 48 rail profiles).

The main characteristics of the applied **adhesive materials** are summarized in Table 1. It should be mentioned that the adhesive type 'B' is a common adhesive material at the Austrian State Railways (ÖBB) for glued insulated rail joint with steel fishplates. Hence the adhesive type 'A' ensured significant high shear strength capabilities during the authors' previously carried out laboratory tests [46].

Table 1 Main characteristics of the applied adhesive materials

Adhesive type	Text details	Installation temperature [°C]	Open time [min]	Bonding/drying time [min]
'A'	Two-component polyurethane sealant and adhesive. Thixotropic. Binding mechanism: poly-addition. Gluing for up to 5.0 mm thickness layers.	+15…+35	10	60
'B'	Two-component methyl methacrylate based adhesive. Gluing for up to 5.0 mm thickness layers.	+15…+30	13	720

3.2.2. Main characteristics of the axial pulling tests

Glued insulated rail joints have to bear very high axial forces in CWR tracks due to change of temperature of the rails compared to the so-called neutral rail temperature. In this case the German method [27] is applied for construction of CWR track (i.e. long rails mainly with rail welding connecting them). Neutral rail temperature is 'set' during the last rail welding, and it means the rail temperature during this procedure. The neutral temperature range (the allowed interval) is almost between +15 °C and +28 °C. There are three neutral temperature values related to a railway track section that is CWR track: (i) neutral temperature of left rail; (ii) neutral temperature of right rail; (iii) neutral temperature of the track that is calculated as the average value of the previous two values. As above mentioned, these values are only related to a tracks section, not the whole railway line. These values are changing due to the expansion and the contract(ion) of the rails and the lateral movements of the track in the ballast bed, in summer and in winter, respectively. The difference between the real rail temperature values and the neutral rail temperature values is the basis of the calculation of the axial force (as well as axial stress) in rails due to temperature change. It is only one part of the reasons for occurrence of this kind of inner force (stress) in the rails, but it is one of the most relevant parts as well. In the case of the Hungarian climate condition, the highest considered rail temperature is +60 °C, the lowest is –30 °C. It means that in the summer a relatively high axial compression force (as well as stress) can be formed and so can, in the wintertime, a relatively high tensile force (as well as stress).

Eqs. (1) and (2) give the formulas for calculation of the above mentioned force and stress value.

$$F_{axial,temp.} = \alpha_{steel} \cdot E_{steel} \cdot A_{rail} \cdot \Delta T_{rail} \tag{1}$$

$$\sigma_{axial,temp.} = \alpha_{steel} \cdot E_{steel} \cdot \Delta T_{rail} \tag{2}$$

where $F_{axial,temp.}$ is the axial inner force in rail (profile) due to change in rail temperature [N], α_{steel} linear thermal expansion coefficient of the rail steel (1.15×10^{-5} 1/°C), E_{steel} is the Young-modulus of rail steel (2.1×10^{11} N/m^2), A_{rail} is the cross sectional area of rail profile [m^2], and $\sigma_{axial,temp.}$ is the normal stress in the rail (profile) due to the change in rail temperature [N/m^2].

The WG18/DG11 pre-standard [39] has a requirement related to the considered value of ΔT_{rail}=50 °C, as well as a safety factor (γ_s=1.5) that has to apply both equations (Eqs. (1) and (2)) as a factor. It means that altogether 75 °C (i.e. 50×1.5) change in rail temperature has to be taken into consideration during the calculations. The authors decided that the inner force and stress values are also determined for 90 °C (the difference between +60 °C and –30 °C; according to D.12/H [43]) change in rail temperature. Table 2 contains all the important parameters and their calculated values as well.

Table 2 Ultimate axial tensile forces, gap opening at ultimate axial tensile forces, as well as gap opening resistance values of specimens, during axial pulling tests [39]

Rail profile	A_{rail} [m^2]	$F_{axial,temp.} \times \gamma_s$ [MN] (ΔT_{rail}=50 °C; γ_s=1.5)	$F_{axial,temp.}$ [MN] (ΔT_{rail}=90 °C)
MÁV 48	0.006292	1.13964	1.36757
54E1 (UIC54)	0.006977	1.26371	1.51645
60E1 (UIC60)	0.007670	1.38923	1.66707

In Fig. 4 the principle arrangement of the axial pulling test is represented. The structure that was applied for the axial pulling tests is very strange equipment because the authors had to solve the main problem of the test procedure: the application of high axial forces. In this case tensile force is loaded onto the rail joint and this force has to be symmetrical just as it should act in the mass point of the rail joint. Because the application of tensile force with this high value is significant and complicated, the authors decided that compression force(s) will be transformed to tensile force(s). Four steel cantilevers were needed for it, namely, those that are fixed to the rail joints' end with high strength fishplate bolts (M27, 8.8). These cantilevers have additional cross-horizontal screws (8 pieces: 4 pieces on the top (Fig. 3) and 4 pieces on the bottom side of the structure). These bolts bear a relatively high bending moment due to the eccentric loading by hydraulic jacks/pistons. During the tests, the loading force and the gap opening are measured and recorded.

Fig. 3 Test set-up of axial pulling test

The main parameters of the test and the test set-up are summarized in Table 3.

It has to be noted that the glued insulated rail joints with only glass-fiber reinforced fishplates were tested, but there were also insulated rail joints assembled by glass-fiber reinforced fishplates (i.e. without adhesive).

During the axial pulling tests all of the applied parameters and characteristics were in accordance with the pre-standard WG18/DG11: the environmental parameters (air temperature, humidity, etc.) as well as the other relevant parameters i.e. speed of loading, the value of maximum loading force, etc.

Table 3 Applied parameters during axial pulling tests

Parameters	Value
Length of specimens	~2500 mm
Fishplate bolts	M24 8.8 (in the case of 48 and 54 rail profiles) and M27 8.8 (in the case of 60 rail profile) quality bolts
Fishplate types	MTH-AP type fishplates
Gap	rail end post (4.0 mm) ± 0 mm (this is considered as '0' state)
Adhesive types	type 'A' and type 'B'
Force effort	2×200 tons Hydrafore hydraulic piston (type Hydrafore YG 200100; work range: 0-700 bar)
Measurement of force	with the help/base of hydraulic pressure (700 bar means ~4000 kN, the system was 500 bar, i.e. 500 bar means ~2857.143 kN)
Measurement of displacement	with the help of an inductive transmitter (LVDT) on the rail head (type HBM W50TK; measurement range: ±50 mm; output signal: 80 mV/V; precision: ±0.4%; shift of '0' point: ±0.05%)
Maximum allowed load of the set-up	220.0 tons (~2200 kN) because of the load bearing capacity of the steel cantilevers fix onto the rail joints by bolts)

3.2.3. Main characteristics of the static and dynamic bending tests

The parameters for the vertical static and dynamic 3-point bending tests are summarized in the following paragraphs.

In the first round, laboratory tests were carried out with the use of three rail systems (MÁV 48: in this case 48.5 kg/m; 54E1 and 60E1); altogether 9 pieces of specimens were assembled for these tests. In the reality conducted tests were as below according to the pre-standard WG18/DG11 on every specimen in this order (from point a) to d)). It has to be mentioned that the deflection values were measured and registered at four points (two in the center of the rail joint to avoid and/or minimize errors of measurements due to twisting, and the other two at the ends of the specimens to be able to consider the uplifting effect). All of tested rail joints (9 pieces) with three rail systems were made by two types of adhesives (6 pieces with adhesive type 'A', 3 pieces with adhesive type 'B'). The specimens were glued insulated rail joints with polymer composite fishplates.

a) Static bending tests without break with the consideration of three different support bay length values, before fatigue ('BF'): 1490 mm, 1200 mm and 1000 mm;
b) Fatigue test (i.e. dynamic bending test) with a load cycle of 3.5 million, the considered-applied bay length value was 1200 mm;
c) Static bending test without break with the previously mentioned three different support bay length values, after fatigue ('AF');
d) Static bending test until break (collapse) using of support bay length value of 1490 mm.

In the second round there were more tasks related to additional 3 pieces of specimens (one specimen from each rail profile) which were glued insulated rail joints with polymer composite fishplates:

The static bending tests were carried out without break considering 13 different support bay length values between 900 and 1490 mm with 50 mm steps, before fatigue ('BF'). The loadings consist of two phases: in the first phase, a preload is applied to achieve the desired position of the tested rail joint. In the second phase, the loading was made up to the calculated maximum force (holding it at this value for 2 minutes) and then decreased the force to the unloaded ('0') position (Fig. 4);

Fatigue test with a load cycle 3.5×10^6 in more steps (support bay length value was 1200 mm) for all the three specimens; after every 0.5×10^6 cycles, a static bending test was performed until 3.5 million cycles (i.e. between 0.5 and 3.5 million cycles) without break considering 13 different support bay length values (900...1490 mm), ('AF');

Static bending tests after 3.5 million cycles in the case of support bay length values 600...850 mm considering symmetrical support arrangement as well as in the case of support bay length values 600…950 mm considering asymmetrical support arrangement.

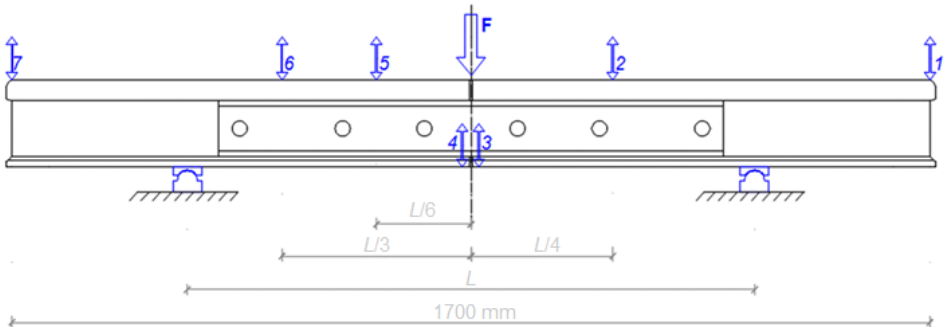

Fig. 4 Set-up of test arrangement of static bending test, supplemented by the position of the applied LVDTs (from 1 to 7)

In the third round in the case of glued insulated rail joints with steel fishplates static bending tests were performed after 3.1 million cycles, then fatigue test with 0.4 million cycles and additional static bending tests after fatigue of 3.5 million cycles. Related to steel fishplated glued insulated rail joints symmetrical and asymmetrical support arrangements were taken into consideration regarding static bending tests.

In the case of second and third rounds the vertical displacement (deflection) values were measured and recorded on the rail head at 7 points. When changing the support bay length values (both symmetrical and asymmetrical support arrangements), the LVDTs (Linear Variable Differential Transformers) are placed in the calculated new position in each case. The deflection values were measured and recorded with a precision of 0.001 mm and an accuracy of 0.4%. In the bending tests (both the static and dynamic ones) there were 3 specimens with polymer composite fishplates and 3 specimens with steel fishplates. In the 3-3 specimens there were 1-1 specimen assembled with the earlier mentioned three rail profiles.

The staff of MÁV-Thermit Ltd. prepared all the glued insulated rail joint specimens in order to conduct laboratory bending tests. Each of the rails was cut to a length of nearly 85 cm, i.e. the total length of the rail joint was 1700 mm). In order to make them able for comparison, in the second round the specimens were tested without application of adhesive materials. These measurements were carried out only related to three different support bay length values (1000, 1200 and 1490 mm).

All of the bending tests were performed considering test parameters in accordance with the standard WG18/DG11 [39].

The requirements for frequency (f) of the dynamic bending test is 3…10 Hz; the considered $F_{vert.,min.}$=5 kN, $F_{vert.,max.}$ can be calculated regarding the methodology shown in the following paragraphs, 3×10^6 loading cycles, the temperature of the structural elements during the tests must not exceed 50 °C.

Using Eqs. (3) and (4) the considered maximum vertical loading force can be calculated.

$$M_r = \sqrt{0.125 \cdot \gamma_c \cdot (Q \cdot E_{steel} \cdot I_{rail} \cdot w_{\max})} \tag{3}$$

$$F_{vert.,max.} = 4 \cdot \frac{M_r}{L} \tag{4}$$

where M_r is the considered bending moment according to pre-standard WG18/DG11 [Nm]. γ_c is the safety and correction factor (1.5 for suspended joints), Q is the static wheel load (×125 kN), I_{rail} is the inertia moment of the rail cross-section with respect to the horizontal axis [m^4], w_{max} is the maximum deflection (vertical displacement) of the glued insulated rail joint (×1.5 mm), $F_{vert.,max.}$ is the maximum vertical loading force [kN] and L is the support bay length value [m].

Table 4 contains the effective maximum loading force values that are taken into consideration in the calculations. They differ from the values calculated by using Eqs. (1) and (2) because parameter M_r was determined in a modified method. Table 4 shows the M_r values recommended by pre-standard WG18/DG11, but the authors changed them a little bit, using the Zimmermann-Eisenmann calculation method [26] considering LM71 type vehicle load 4×250 kN with a vehicle axle space of 1.60 m [47]. During the calculation the authors considered the following parameters:

- static axle load, $2\times Q$=250 kN;
- distance of axles (axle space); x=1.60 m;
- speed; V=160 km/h (in the case of 54 and 60 rail profiles);
- speed; V=100 km/h (in the case of 48 rail profile);
- probability is 99.7%; t=3 (Student-distribution);
- track condition; φ=0.15 (average);
- effective length of half sleeper; ℓ=950 mm;
- effective with of half sleeper; b=300 mm;
- considered sleeper space; k=1200 mm (a non-supported sleeper is taken into consideration, k=2×600 mm=1200 mm);
- bedding modulus; C=0.10 N/mm^3;
- dynamic amplificator factor; DAF=1.714 (in the case of 54 and 60 rail profiles);
- dynamic amplificator factor; DAF=1.285 (in the case of 48 rail profiles);
- characteristic length; L_{ch}=1014.656 mm (in the case of 60 rail profile);
- characteristic length; L_{ch}=949.834 mm (in the case of 54 rail profile); and,
- characteristic length; L_{ch}=882.346 mm (in the case of 48 rail profile).

The other details of the calculation are not published; the result of the modified bending moment values (M_r) to be considered are 42.63; 40.85 and 34.71 kNm, related to 60; 54 and 48 rail profiles, respectively.

Based on the considered modified bending moment values, calculated $F_{vert.,max.}$ values are determined; they can be seen below (they are only detailed related to L=1.2 m; the other calculation can be performed using Eq. (4)): 142.00; 136.20 and 115.70 kN, related to 60; 54 and 48 rail profiles, respectively.

As an example a bending moment graph is given in Fig. 5 based on the calculated data.

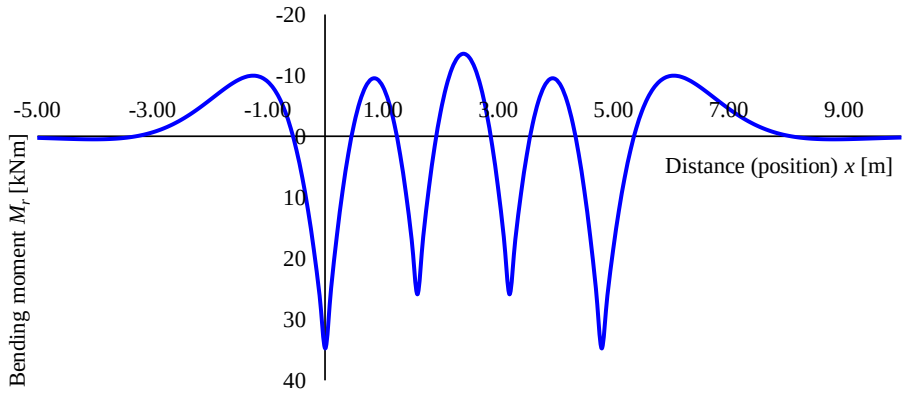

Fig. 5 Bending moment vs. longitudinal position diagram (rail profile: MÁV 48; calculation method: Zimmermann-Eisenmann; LM71 vehicle load; maximum positive bending moment M_r=+34.71 kNm at x=0.00 m and x=4.80 m positions)

The LVDTs during static bending tests were HBM W50TK types (measurement range: ±50 mm; output signal: 80 mV/V; precision: ±0.4%; shift of '0' point: ±0.05%) (see Fig. 4).

During the static and dynamic bending tests all of the applied parameters and characteristics were in accordance with the pre-standard WG18/DG11 [39]: the environmental parameters (air temperature, humidity, etc.) as well as the other relevant parameters, i.e. speed of loading, etc.

4. Results

4.1. Results of the axial pulling tests

In the case of the axial pulling tests the gap opening parameter was the most important to be analyzed.

In Figs. 6 and 7 the variation of axial pulling (tensile) force as a function of gap opening values is represented related to all the tested rail joints.

In the legends of Figs. 6 and 7, the numbers 48, 54 and 60 mean the rail system (rail profile) of the rail joints, letter 'A' and 'B' are related to the type of the applied adhesive material (type 'A' and 'B', respectively), 'WG' means 'without gluing'.

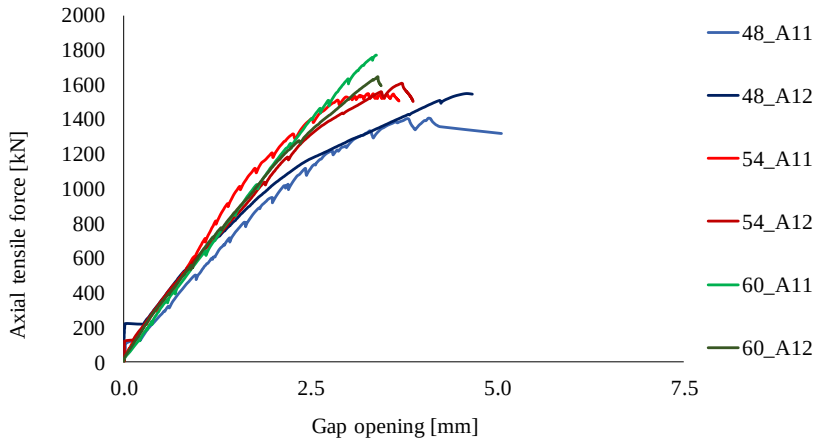

Fig. 6 Axial tensile force vs. gap opening diagram 1

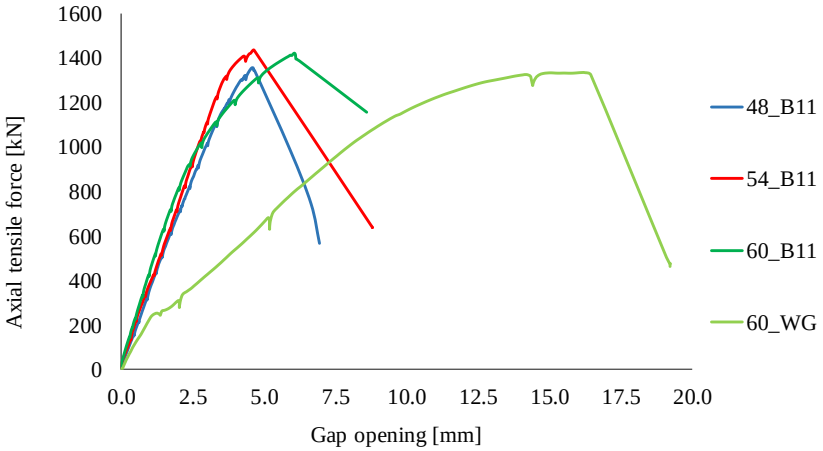

Fig. 7 Axial tensile force vs. gap opening diagram 2

The authors examined axial tensile force values at 0.1 mm gap opening (initial state). The results showed that the bolts and the adhesive material worked adequate. On the basis of the measurements the following statements can be formulated.

In the case of specimens assembled with 48 rail profiles the adhesive type ‘A’ ensured approximately 1.8 to 2.7 times higher initial axial tensile force values than the specimens produced with adhesive type ‘B’ (124 and 185 kN, as well as 68 kN, respectively) at 0.1 mm gap opening, the gap opening values were approx. 5 mm at the ultimate axial tensile forces.

Regarding specimens with 54 rail profiles and adhesive type ‘A’ provided approx. 1.7 to 2.1 times higher axial tensile forces than ones with adhesive type ‘B’ at 0.1 mm gap opening value, the final gap opening was 20% higher in the case of specimens with adhesive type ‘B’ than with type ‘A’.

In the case of specimens assembled with 60 rail profiles the measured axial tensile forces at 0.1 mm gap opening were nearly the same, but compared to the ultimate tensile

force values they were only their 0.037-0.047%. It means that the rail joints opened at relatively low loading states and the 4.0±0 mm gap evolved at the beginning of the tests. The maximum gap opening value of specimens made with adhesive type 'A' was approx. 3.4 mm. In the case of specimens 'WG' the axial initial gap opening (0.1 mm) developed at even 17 kN, the ultimate gap opening value was approx. 16 mm. Regarding specimen 60_A11 (it was the first measured specimen) the break did not occur even for the third trying; in the case of the first and the second trying the M27 8.8 bolts (that fixed the loading cantilevers to the rail joint specimen) were sheared, the specimen was able to bear the required axial tensile force.

The gap opening resistance (unit kN/mm) was calculated related to all of the specimens. This parameter characterizes the stiffness of the glued insulated rail joint against gap opening at a given tensile force. The higher the gap opening resistance, the lower the evolved gap at the same tensile force is, i.e. at a given force interval. This parameter has to be determined for the constant tangent section of the loading diagrams. Table 4 shows not only the gap opening resistance values representing the tested specimens, but the ultimate axial tensile forces as well as the gap opening values at these ultimate loading force values.

Table 4 Ultimate axial tensile forces, gap opening at ultimate axial tensile forces, as well as gap opening resistance values of specimens, during axial pulling tests

Designation of specimen	Ultimate axial tensile force [kN]	Gap opening at ultimate axial tensile force [kN]	Calculated gap opening resistance [kN/mm]
48_A11	1317.30	5.050	460.64
48_B11	1346.00	4.650	344.72
48_A12	1547.20	4.606	499.85
54_A11	1547.20	3.603	582.03
54_B11	1433.90	4.653	369.13
54_A12	1605.30	3.725	535.57
60_A11	1767.80	3.378	556.60
60_B11	1420.90	6.069	383.96
60_A12	1645.10	3.406	545.62
60_WG	1332.20	16.106	146.96

Based on the obtained results (see Figs. 6 and 7 as well as Table 4) it can be concluded that the specimens had practically very low (or almost no) resistance in the initial intervals, although better for specimens made using adhesive type 'A'). This statement is true not only for glued specimens, but the non-glued ('WG') one. It means that approx. only the 0.04% of the ultimate axial tensile forces can be obtained at 0.1 mm gap opening. It has to be noted that the higher the gap opening, the higher the risk for failure of glued insulated rail joints is; it can happen earlier during railway operation. The question can be formulated why adhesive material in rail joints is applied if these joints do not have better behavior against gap opening at the initial stage. (It has to be noted that rail joints with adhesive material will have significantly better behavior during the lifetime under a repeated loading.)

The axial tensile stresses were then determined and plotted into Fig. 8 The data (stress values) are related to the center line of the rail joint (taking into account the cross-sectional area of the fishplate pair).

Of course, the ‘style’ and the ‘appearance’ of the axial tensile force and axial tensile stress diagrams are almost the same, but the different cross-sectional area of the fishplates (i.e. related to rail profiles 48, 54 and 60) influences the peak values as well as the tangent of the curves. These stress values are important; they can be compared to the limit values related to the base material. It has to be noted that higher normal stress values evolved in the fishplates due to the reduced cross-sectional area considering the bolt holes. These stress values 51.6%, 42.3% and 36.2% higher than in Fig. 8 (related to 48, 54 and 60 rail profiles, respectively). (The effective cross sectional areas are 6416 and 4232 mm^2; 7346 and 5162 mm^2; as well as 8212 and 6028 mm^2; related to the non-weakened and the weakened cross-sections and 48, 54 and 60 rail profiles, respectively).

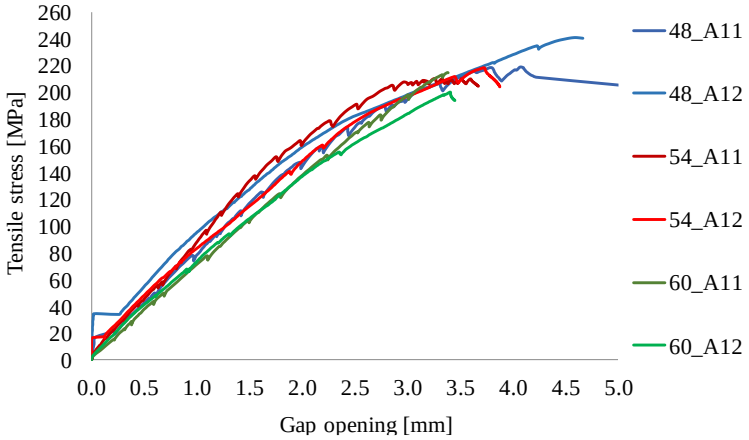

Fig. 8 Axial tensile stress vs. gap opening diagram

4.2. Results of the static and dynamic bending tests

In this paragraph only the relevant results are introduced. Because of many measurements related to many aspects and many specimens, the authors collected some of the main results which represent the behavior of the investigated glued insulated rail joints. In every figure in this paragraph the abbreviation ‘BF’ means ‘before fatigue’, ‘AF’ means ‘after fatigue’. Where there is not any supplementary information next to ‘AF’ abbreviation, it is related to 3.5 million loading cycle. There are a lot of new introduced calculated parameters which are adequate for evaluation of glued insulated rail joints. In every case they are explained and they are combined and represented by unique diagrams, graphs, or maybe tables.

The authors examined and calculated the deterioration rate of the specimens considering the carried out laboratory dynamic bending tests with the fatigue interval up to 3.5 million cycles, supplemented by static bending tests before and after the fatigue steps. These evaluations are based on the assessment of the variation of vertical deflection values of the specimens as a function of fatigue (loading) cycles. The values are able to be compared to the initial values considering each specimen, this initial value (‘0’ state) is the measured state and bending behavior of the specimens (during static bending tests). The calculations were carried out related to bending tests with support bay length values of 1000, 1200 and 1490 mm, and the examined three rail profiles (48, 54 and 60) were taken into account.

Linear regression lines were plotted into all of the vertical load vs. deflection functions (diagrams), i.e. linear regression functions were calculated to relevant intervals. The main parameter of these linear regression functions is the tangent (slope) in kN/mm unit. During the calculations the averages of the vertical deflection values were considered related to the maximum vertical loading force at the middle-bay position, regarding each rail profile and each fatigue step. The determined so called 'stiffness of rail joint' parameter (its unit is kN/mm/m) considers the support bay length values. They were compared to the initial measurements that are related to the 'before fatigue' states.

In Table 5 the measured peak (ultimate) vertical force values, the peak (ultimate) bending moment are collected. The safety factor is 1.5 in the calculations.

Table 5 Ultimate vertical force, ultimate bending moment as well as the calculated bending moment values considering safety factor, during the static bending tests until break (the support bay length value is 1490 mm)

Designation of specimen	Ultimate (peak) vertical force [kN]	Ultimate (peak) bending moment [kNm]	Calculated bending moment considering safety factor [kNm]
48_A1	196.32	73.13	52.065
48_B1	230.28	85.78	52.065
48_A2	244.68	91.14	52.065
54_A1	294.60	109.74	61.275
54_B1	240.24	89.49	61.275
54_A2	306.00	113.98	61.275
60_A1	308.52	114.92	63.945
60_B1	334.32	124.53	63.945
60_A2	430.08	160.20	63.945

In Fig. 9 the variation of stiffness of rail joint is represented. Fig. 10 gives examples for variation of the stiffness of the rail joint parameter as a function of support bay length between 900 and 1490 mm.

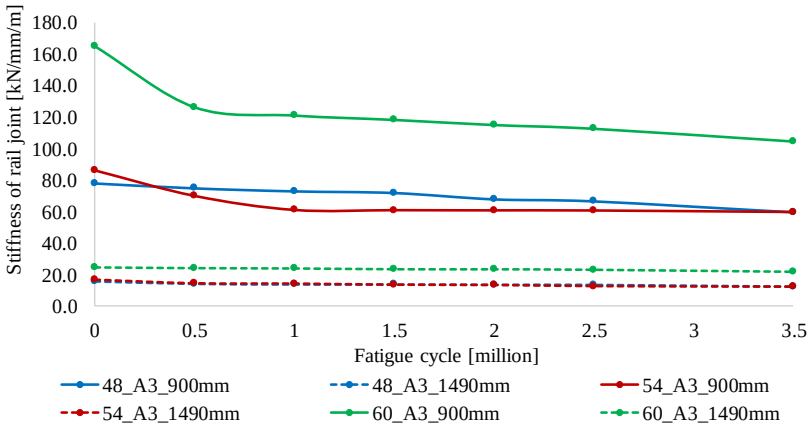

Fig. 9 Stiffness of rail joint vs. fatigue cycle diagrams; 48, 54, 60 rail profiles and 900 and 1490 mm support bay length values

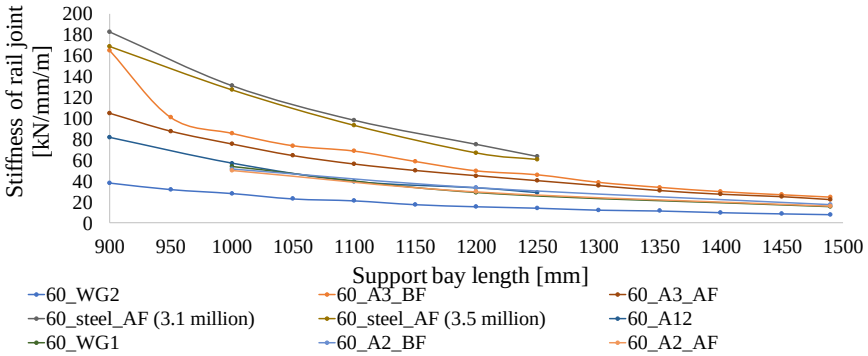

Fig. 10 Stiffness of rail joint vs. support bay length; 60 rail profile

Fig. 11 shows a newly introduced parameter, the so-called 'stiffness ratio'. This parameter characterizes the rail joints compared to the initial state (i.e. 'BF') of the examined glued insulated rail joints; it means the stiffness ratio is 1.0 at 0.0 million fatigue cycle, related to all the investigated rail joints with each rail profile (48, 54 and 60). The values that are represented in Fig. 11 are average values of the stiffness of rail joints; the considered values in the calculation of average are related to 900 and 1490 mm support bay length values. There are two relevant phases in each graph. The first part is between 0.0 and 0.5 million fatigue cycles, the second part is related to between 0.5 and 3.5 million fatigue cycles. In this second phase linear regression functions were determined which have relatively high R^2 coefficient (>.94).

Table 6 represents the 'deterioration speed' parameter related to specimens with 48 rail profile, its unit is kN/mm/m/fatigue cycle. It is calculated on the basis of 'stiffness of rail joint' (unit: kN/mm/m). In the 'deterioration speed' the number of fatigue cycles is also considered. Actually it is the tangent of the calculated line of the 'stiffness of rail joint' between 0.0 and 3.5 million points (it is not regression line).

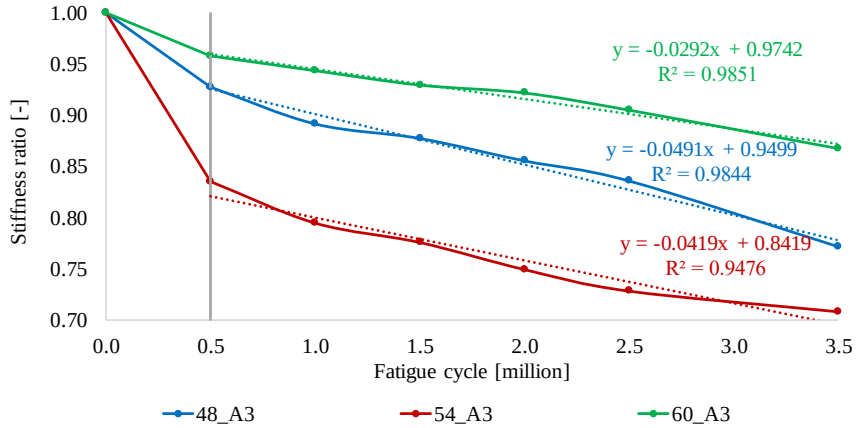

Fig. 11 Stiffness ratio diagrams in the case of 48, 54, 60 rail profiles calculated from the average of stiffness of rail joints (900 and 1490 mm)

Table 6 Deterioration speed values of 48 rail profile specimens

Designation of specimens	Deterioration speed [kN/mm/m/fatigue cycle]
48_A1_1000 mm	–0.070
48_B1_1000 mm	–0.032
48_A2_1000 mm	–0.137
48_A1_1200 mm	–0.055
48_B1_1200 mm	–0.041
48_A2_1200 mm	–0.143
48_A1_1490 mm	–0.055
48_B1_1490 mm	–0.023

Fig. 12 contains a graph related to (vertical) deformation line of glued insulated rail joint (with 48 rail profile) measured by 7 pieces of LVDTs fixed on the rail head during static bending tests, in the case the support bay length value is 900 mm. The plotted graphs given in Fig. 12 refer to the vertical deflection values related to the considered maximum vertical loading force (calculated from the Zimmermann-Eisenmann method see Chapter 3.2.3 and [26]) Of course, the measurements are available for each support bay length value and all of the considered and tested three rail profiles.

In Fig. 13 another special, new parameter is shown. It is the so-called 'deflection parameter' and it is determined in mm^2 unit. This parameter is calculated as the integral (area) below the deflection line in the whole length of the rail joints. There are two phases in each graph. The first part is between 0.0 and 0.5 million fatigue cycles, the second part is related to between 0.5 and 3.5 million fatigue cycles. In this second phase linear regression functions were determined which have relatively high R^2 coefficient (R^2>0.80).

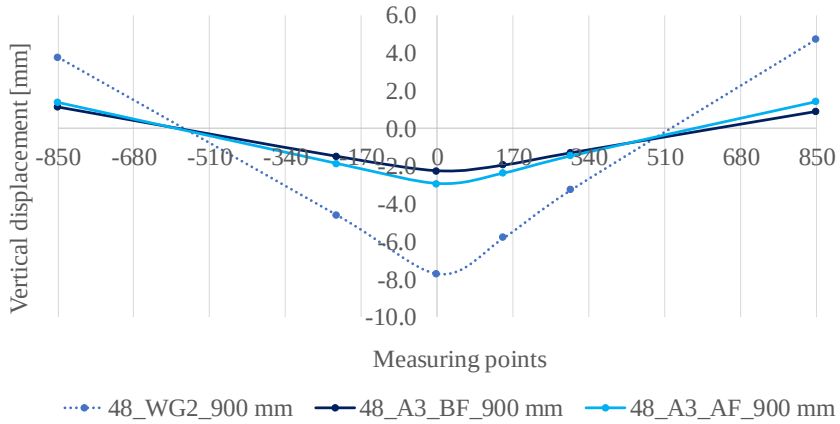

Fig. 12 Measured deformation line of insulated rail joints assembled by polymer composite fishplates with and without gluing in the case of 900 mm support bay length, as well as 48 rail profile

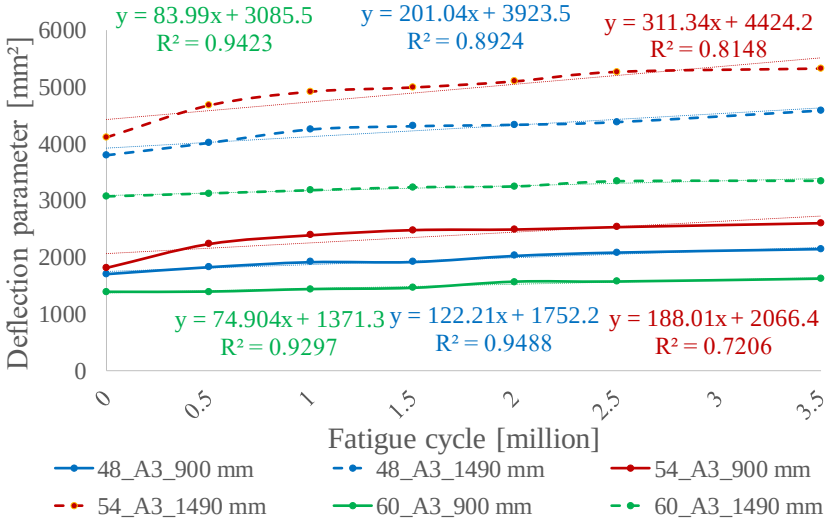

Fig. 13 Deflection parameters vs. fatigue cycle

5. CONCLUSIONS

The authors formulated theses that can be read in the following paragraphs based on the results in Chapter 4. In the first part they phrased the statements related to static and dynamic bending tests while in the second part there are statements related to axial pulling tests.

The authors proved that there are two, well-separated sections, phases in the stiffness ratio vs. fatigue cycle functions related to the tested, investigated glued insulated rail joints assembled by glass-fiber reinforced fishplates. There is a border line between the two phases at the 0.5 million fatigue cycle value. In the second phase the deterioration (variation) can be characterized by linear regression functions that have significant R^2 coefficients.

The authors introduced parameters connected to the static and dynamic bending tests of glued insulated rail joints in laboratory. These are the 'stiffness of rail joint' [kN/mm/m], the 'deterioration speed' [kN/mm/m/fatigue cycle], that can help with the evaluation and comparison of the tested glued insulated rail joints. The authors stated the variation of stiffness of rail joints related to the examined glued insulated rail joints made by glass-fiber reinforced and steel fishplates as a function of fatigue cycle. In the case of polymer composite fishplated glued insulated rail joints these variation speed (the tangent of stiffness of rail joint graphs as a function of fatigue cycle) is 1.17%, 2.16% and 8.54% higher compared to the tested steel fishplated glued insulated rail joints related to the 60, 54 and 48 rail profiles, respectively. The types of fishplates are MTH-AP and MTH-P (polymer composite and steel, respectively). The integral function of the deflection graphs (i.e. the area 'below' the deflection graphs) was determined as a function of support bay lengths; they are adequate to assess the whole deformation line of the holding device (i.e. the glued insulated rail joint) in the vertical plane. The variation of these integral functions are proved that it can be characterized by quadratic polynomial regression functions in any cases (R^2>0.97). Based on performed calculations the authors stated that the previously

mentioned integral value is 1.27%, 1.91% and 1.61% higher in the case of glued insulated rail joints with glass-fiber reinforced fishplates than ones with steel fishplates (related to 60, 54 and 48 rail profiles, respectively). The last statements mean (in the case the vertical deflection values at middle-bay are known) that the deformation lines of glued insulated rail joints with polymer composite fishplates are close to a symmetric triangle shape while the steel fishplated ones' deformation lines are close to a beam without joint (i.e. they have quadratic parabola shapes).

Based on the axial pulling tests it is proved that adhesive type 'A' ensured an average 10% higher 'gap opening resistance' than adhesive type 'B' in the case of glued insulated rail joints assembled by glass-fiber reinforced fishplates (the effective values are 10.96%, 9.74% and 9.00% related to 60, 54 and 48 rail profiles, respectively). The adhesive type 'A' can be applied more universal in the case of the tested rail joints; in the case of using of adhesive type 'B' the axial pulling graphs spectacularly differ just as they guaranteed higher deviation related to the peak axial tensile stresses (and forces).

The authors would like to summarize the experiences not only of their laboratory tests, but tests on site, too, because this paper is considered as a concluding article.

Based on the conducted laboratory [46, 48] and tests on site [49] some relevant statements can be drawn which are able to be useful for the application of MTH-AP fishplated in glued insulated rail joints:

- The behavior and service life of the polymer composite fishplated glued insulated rail joints depend significantly on the accuracy of the preparation of the rail joint. When mounting, no gap is allowed between the end of the rail and the end of the rail end post on either side.
- Those adhesive types that can only be used in thick layers are not suitable for gluing the rail end post to the end of the rail because the thick layer is able to pug due to traffic (passing wheels) after a relatively short time.
- High attention has to be given to the surface and surface design of polymer composite fishplates because the adhesive material may not be able to adhere sufficiently to lacquered and/or surface-coated fishplates.
- The fishplates have to fit exactly within specified tolerances to the rail web.
- The required torque for fishplate bolts is min. 850 Nm.
- The applicable support set-up of track considering glued insulated rail joint is suspended joint.
- Min. 3-3 pieces of supporting sleepers next to the glued insulated rail joints have to be tamped carefully, unsupported sleepers are not allowed.
- The appearance of 'whitening' visible to the eyes in the lower part of the joint (i.e. fishplates), even in the middle, makes it likely that the fishplate crack will develop nearby. The crack in the fishplate is not followed by a sudden fracture (break), it increases slowly with the repetition of the load. The cracked fishplate must be replaced.
- In the case of glued insulated rail joints with MTH-AP fishplates, the allowed static axle load is 225 kN and the allowed speed is up to 160 km/h (for 54 and 60 rail profile), as well as 100 km/h (for 48 rail profile).
- The rail temperatures during installation should be taken into account in accordance with MÁV regulation D.12/H [43].
- The relaxation of CWR tracks has to be performed according to MÁV regulation D.12/H [43].

- Production of glued insulated rail joints assembled by MTH-AP fishplates is preferred in factory, not on-site.
- The fishplate bolts should be min. 10.9 strength quality.
- The connecting cut (trim) of the rails should be perpendicular to the longitudinal axis of the rail. The inclined cut is not preferred.
- The application of heat-treated or special rail steel categories is preferred, but not prescribed.
- In the case of structural ballast gluing is planned for the glued insulated rail joint, it is necessary to consult with the owners of the patent law.

6. Summary and Further Research Possibilities

This article summarizes the research carried out in the topic of glued insulated rail joints assembled by glass-fiber reinforced (polymer composite) fishplates. The authors introduced their own performed laboratory tests, as well as the relevant results and the connecting evaluations and recommendations for application.

The results were formulated as theses, which were drawn as scientific statements.

At the end of the article, the authors drew relevant statements, main aspects and recommendations related to application of MTH-AP (produced by Russian company, APATECH) based on the conducted laboratory tests as well as on-site tests and their results.

It has to be mentioned that since 2016 there are four testing (experimental) sites in the international main railway line No. 1 in Hungary (Kelenföld-Hegyeshalom state border). These glued insulated rail joints work well, no special problems there were related to them [38, 49].

The authors formulate some further, research possibilities in this topic:

- Application of computer tomography related to the laboratory tests (i.e. axial pulling tests, as well as static and dynamic bending tests) to be able to assess the changing of fishplates' inside material structure regarding fatigue cycles.
- There are possibilities for evaluating the deformation characteristics and their changing of fishplates. These technologies are the measurements by GOM ARAMIS, GOM TRITOP [50], as examples.
- Special 2D/3D FE modeling of fishplates as well as the whole rail joint.
- Continuation of diagnostics and the data processing of field tests (i.e. measurements made by railway track geometry recording cars).
- Taking into consideration of rail and wheel wear due to GIRJs.
- Paying respect to application of fuzzy and fuzzy-random logics or neural networks during assessment of field tests.

Acknowledgements: *The authors would like to thank for the support of MÁV (Hungarian State Railways), MÁV-THERMIT Ltd., as well as Universitas-Győr Nonprofit Ltd. The authors have much to be thankful to Dénes Szekeres who was the responsible employee of the MÁV during the related R&D.*

REFERENCES

1. Jahangiri, M., Zakeri J.-A., 2019, *Dynamic Analysis of Two-lane Skewed Bridge and High-speed Train System*, Periodica Polytechnica Civil Engineering, 63(3), pp. 695-708.
2. Csortos, G., Augusztinovicz, F., Kazinczy, L., 2020, *Examination of Rail Dampers with Respect to Noise and Vibration Mitigation*, Periodica Polytechnica Civil Engineering, 64(3), pp. 658-667.
3. Kuchak, A.T.J., Marinkovic, D., Zehn, M., 2020, *Finite element model updating - Case study of a rail damper*, Structural Engineering and Mechanics, 73(1), pp. 27-35.
4. Kuchak, A.T.J., Marinkovic, D., Zehn, M., 2021, *Parametric Investigation of a Rail Damper Design Based on a Lab-Scaled Model*, Journal of Vibrational Engineering and Technologies, 9(1), pp. 51-60.
5. Plasek, O., Hruzikova, M., 2017, *Under sleeper pads in switches & crossings*, IOP Conference Series: Materials Science and Engineering, 236(1), 012045.
6. Plasek, O., Hruzikova, M., Svoboda, R., Vendel, J., 2015, *Influence of under sleeper pads on track quality*, Akustika, 23, pp. 28-33.
7. Sysyn, M., Gerber, U., Nabochenko, O., Dehne, S., 2020, *A Laboratory Study of Pressure Distribution and Residual Settlements in Wide Grading Double Layer Railway Ballast under Long-Term Cyclic Loading*, Archives of Civil Engineering, 64(2), pp. 561-578.
8. Gerber, U., Sysyn, M., Zarour, J., Nabochenko, O., 2019, *Stiffness and strength of structural layers from cohesionless material*, Archives of Transport, 49(1), pp. 59-68.
9. Przybylowicz, M., Sysyn, M., Kovalchuk, V., Nabochenko, O., Parneta, B., 2020, *Experimental and Theoretical Evaluation of Side Tamping Method for Ballasted Railway Track Maintenance*, Transport Problems, 15(3), pp. 93-106.
10. Sysyn, M., Nabochenko, O., Kovalchuk, V., Przybyłowicz, M., Fischer, S., 2021, *Investigation of interlocking effect of crushed stone ballast during dynamic loading*, Reports in Mechanical Engineering, 2(1), pp. 65-76.
11. Sysyn, M., Nabochenko, O., Kovalchuk, V., 2020, *Experimental investigation of the dynamic behavior of railway track with sleeper voids*, Railway Engineering Science, 28, pp. 290-304.
12. Kurhan, M., Kurhan, D., Novik, R., Baydak, S., Hmelevska, N., 2020, *Improvement of the railway track efficiency by minimizing the rail wear in curves*, IOP Conference Series: Materials Science and Engineering, 985, 012001.
13. Fischer, S., 2017, *Breakage Test of Railway Ballast Materials with New Laboratory Method*, Periodica Polytechnica Civil Engineering, 61(4), pp. 794-802.
14. Juhász, E., Fischer, S., 2019, *Investigation of railroad ballast particle breakage*, Pollack Periodica, 14(2), pp. 3-14.
15. Benmebarek, A.M., Movahedi, R.M., 2021, *DEM Modeling of Crushable Grain Material under Different Loading Conditions*, Periodica Polytechnica Civil Engineering, doi: 10.3311/PPci.17948.
16. Czinder, B., Vásárhelyi, B., Török, Á., 2021, *Long-term abrasion of rocks assessed by micro-Deval tests and estimation of the abrasion process of rock types based on strength parameters*, Engineering Geology, 282, 105996.
17. Šestaková, J., Ižvolt, L., Mečár, M., 2019, *Degradation-Prediction Models of the Railway Track Quality*, Civil And Environmental Engineering Reports, 15(2), pp. 115-124.
18. Šestáková, J., Pultznerová, A., 2021, *Diagnostics data in the framework of railway tracks maintenance*, IOP Conference Series: Materials Science and Engineering, 1015(1), 012062.
19. Kurhan, M., Kurhan, D., Husak, M., Hmelevska, N., 2020, *The Advisability of Using Dual Gauge for Expansion of the International Traffic*, Transport Means 2020, Kaunas, Lithuania, pp. 469-474.
20. Kurhan, M.B., Verbitskii, V.G., Kurhan, D.M., 2019, *Difference Research of Ukrainian and European Railway Infrastructure*, Nauka ta Progres Transportu, 83(5), pp. 52-70.
21. Kampczyk, A. Dybeł, K., 2021, *Integrating surveying railway special grid pins with terrestrial laser scanning targets for monitoring rail transport infrastructure*, Measurement, 170, 108729.
22. Kampczyk, A., 2020, *Measurement of the geometric center of a turnout for the safety of railway infrastructure using MMS and total station*, Sensors, 20(16), 4467.
23. Kampczyk, A., 2020, *An Innovative Approach to Surveying the Geometry of Visibility Triangles at Railway Level Crossings*, Sensors, 20(22), 6623.
24. Blagojević, A., Stević, Ž., Marinković, D., Kasalica, S., Rajilić, S., 2020, *A novel entropy-fuzzy PIPRECIA-DEA model for safety evaluation of railway traffic*, Symmetry, 12(9), 1479.
25. Prastowo, T.Y, Purba, H.H., 2020, *Risk management on railway projects: a literature view*, Facta Universitatis: Mechanical Engineering, 18(3), pp. 231-240.
26. Esveld, C., 2014, *Modern railway track*, MRT Production, Zaltbommel (Netherland), 653 p.
27. Gajári, J., 1983, *Vasútépítéstan I.*, Tankönyvkiadó, Budapest (Hungary), 428 p.

28. Kurhan, M.B., Kurhan, D.M., 2016, *Features of perception of loading elements of the railway track at high speeds of the movement*, Nauka ta Progres Transportu, 56(2), pp. 136-145.
29. Ha, G.X., Marinkovic, D., Zehn, M.W, 2019, *Parametric investigations of mechanical properties of nap-core sandwich composites*, Composites Part B: Engineering, 161, pp. 427-438.
30. Rama, G., Marinkovic, D., Zehn, M., 2018, *High performance 3-node shell element for linear and geometrically nonlinear analysis of composite laminates*, Composites Part B: Engineering, 151, pp. 118-126.
31. Gallou, M., Temple, B., Hardwick, C., Frost, M., El-Hamalawi, A., 2018, *Potential for external reinforcement of insulated rail joints*, Proceedings of the Institution of Mechanical Engineers, Part F: Journal of Rail and Rapid Transit, 232(3), pp. 697-708.
32. Beaty, P., Temple, B., Marshall, M.B, Lewis, R., 2016, *Experimental modelling of lipping in insulated rail joints and investigation of rail head material improvements*, Proceedings of the Institution of Mechanical Engineers, Part F: Journal of Rail and Rapid Transit, 230(4), pp. 1375-1387.
33. Lewis, S.R., Lewis, R., Goodwin, P. S., Fretwell-Smith, S., Fletcher, D. I., Murray, M., Jaiswal, J., 2017, *Full-scale testing of laser clad railway track; Case study – Testing for wear, bend fatigue and insulated block joint lipping integrity*, Wear, 376–377, Part B, pp. 1930-1937.
34. Mandal, N.K., 2014, *On the low cycle fatigue failure of insulated rail joints (IRJs)*, Engineering Failure Analysis, 40, pp. 58-74.
35. Mandal, N.K., 2014, *Ratchetting of railhead material of insulated rail joints (IRJs) with reference to endpost thickness*, Engineering Failure Analysis, 45, pp. 347-362.
36. CRC for Rail Innovation, 2009, *Review of insulated rail joint*, Available at: https://pdfs.semanticscholar.org/7c15/18810a7a6f19100d9c90a3aa7f0ffb4bd4ef.pdf (last access: 28.03.2021)
37. Stephen, J.T., Hardwick, C., Beaty, P., Marshall, M.B., Lewis, R., 2018, *Ultrasonic monitoring of insulated block joints*, Proceedings of the Institution of Mechanical Engineers, Part F: Journal of Rail and Rapid Transit, 233(3), pp. 251-261.
38. Németh, A., 2020, *A polimer-kompozit hevederes ragasztott-szigetelt sínillesztések alkalmazásának vizsgálata hézagnélküli vasúti vágányokban*, PhD Thesis, Széchenyi István University, Hungary, 218 p.
39. CEN/CENELEC, 2015, *prEN 16843:2015: Mechanical requirements for joints in running rails*, standard (WG18/DG11), Brussels (Belgium).
40. Standards Australia International Ltd., 2002, *AS 1085.12: Railway Track Material, Insulated Joint Assemblies*, from: https://www.saiglobal.com/PDFTemp/Previews/OSH/as/as1000/1000/108512.pdf (last access: 28.03.2021)
41. Austrian State Railways (ÖBB), 2013, *07.09.26: ÖBB Infra – Oberbau // Anforderung an Oberbaukomponenten – Isolierstöße, Technische Lieferbedingungen*, Vienna (Austria).
42. Hungarian State Railways (MÁV), 1998, *PHM. Ig. 402.-P-893/1998. 54 r. műanyag-hevederek alkalmazása*, Budapest (Hungary).
43. Hungarian State Railways (MÁV), 2009, *D.12/H: Hézagnélküli felépítmény építése, karbantartása és felügyelete*, Budapest (Hungary).
44. Hungarian Standard Institution, 2017, *MSZ EN 13674-1:2011+A1:2017: Railway applications. Track. Rail. Part 1: Vignole railway rails 46 kg/m and above*, Budapest (Hungary).
45. Hungarian State Railways (MÁV), 1988, *D.54: Építési és pályafenntartási műszaki adatok, előírások I-II.*, Budapest (Hungary).
46. Németh, A., Fischer, S., 2019, *Laboratory Test Results of Glued Insulated Rail Joints Assembled with Traditional Steel and Fibre-Glass Reinforced Resin-Bonded Fishplates*, Nauka ta Progres Transportu, 81(3), pp. 65-86.
47. Hungarian Standard Institution, 2015, *MSZ EN 1991-1-7:2015 Eurocode 1: Actions on structures. Part 1-7: General actions. Accidental actions*, Budapest (Hungary).
48. Németh, A., Fischer, S., 2018, *Investigation of glued insulated rail joints with special fiber-glass reinforced synthetic fishplates using in continuously welded tracks*, Pollack Periodica, 13(2), pp. 77-86.
49. Németh, A., Fischer, S., 2019, *Field Tests of Glued Insulated Rail Joints with Usage of Special Plastic and Steel Fishplates*, Nauka ta Progres Transportu, 80(2), pp. 60-76.
50. Németh, A., Fekete, I., Szalai, S., Fischer, S., 2019, *Supplementary Laboratory Investigations of Modern Plastic-Polymer Fishplates for Rail Joints*, Nauka ta Progres Transportu, 84(6), pp. 86-102.